Available online at www.sciencedirect.com

ScienceDirect

IFAC PapersOnline CONFERENCE PAPER ARCHIVE

IFAC PapersOnLine 58-2 (2024) 168–173

Optimal Operation of an Innovative Electric Vehicle Charging Hub directly fed by Renewables

Alphonse Francis*, Matteo Fresia*, Stefano Bracco*, Edoardo Barabino**

**Electrical, Electronics, Telecommunications Engineering and Naval Architecture Department, University of Genoa, Genoa, GE 16145, Italy, alphonse.francis@edu.unige.it*

***FERA S.r.l., Piazza Cavour 7, Milan, MI 20121, Italy*

Abstract: The reduction of Green House Gases (GHGs) emissions has been the top priority of the European Union (EU) in recent times. The increase in use of Electric Vehicles (EVs) to combat climate change is viable only with the use of Renewable Energy Sources (RESs) to power them. Since the Paris Agreement in 2015, the integration of RESs into the charging infrastructure has increased in the EU. The increasing market share of EVs in various categories has called for immediate changes in the EV charging infrastructure and in the operation of charging hubs. This paper aims to present an Energy Management System (EMS) to efficiently manage an EV charging hub fed by RESs, reducing the daily costs of operation and GHG emissions. The mathematical model of the EMS is developed in Matlab as a Mixed Integer Linear Programming (MILP) model. The MILP-based EMS is applied to the real-world case of an innovative EV charging hub located in the Ligurian region of Italy and the results of the optimization are reported.

Keywords: MILP, Energy Management System, EV Charging Hub, Renewables, Capability Curves.

1. INTRODUCTION

In order to decarbonize the transportation sector, accounting for nearly 26% of CO_2 emissions in the European Union (EU) as presented by the European Environment Agency (2022), the European Commission has issued the "Fit for 55" package, that targets to reduce the Green House Gases (GHGs) emissions by 40% if compared to the emission level of 2005 in different sectors, including road and domestic maritime transport. The package sets a 55% reduction of CO_2 emissions for new cars and 50% for new vans from 2030 to 2034, while a 100% reduction in CO_2 emissions for both new cars and vans is set from 2035. A surge in the use of Electric Vehicles (EVs) is its outcome, leading to the need for the smart management of the EV charging infrastructure. The use of Renewable Energy Sources (RESs) to meet the increased demand justifies the use of EVs, which has led the EU to accelerate its transition from energy production using imported fossil fuels to local energy production using RESs. The recently revised Renewable Energy Directive (RED III) requires the member states to increase the EU final energy consumption share of RES to at least 42.5% by 2030, if compared to the current 32%. The integration of RESs into the EV charging infrastructures is twofold. On one hand, as reported by Tant et al. (2013), to deal with the inherent uncertainty regarding the availability of the primary source, Energy Storage Systems (ESSs), especially Battery Energy Storage Systems (BESSs), are used in conjunction with RESs to smoothen their power output and avoid rapid voltage and power swings in the network. On the other hand, smart charging strategies for EVs to overcome this uncertainty are available, like overnight charging, destination charging and On-the-Move charging. Solutions like load shifting or smart charging might not be the favourable option for private users, as the EV demand needs to be satisfied at all time periods: this technique has some interest when it can be applied to large EVs fleets.

Various articles related to the design and operation of Microgrids (MGs) with EV charging hubs/stations are available in literature. Pan et al. (2015) describe an Energy Management System (EMS) using model predictive control for the management of a MG with dispatchable and non-dispatchable generation units, ESSs and non-controllable loads. Bracco et al. (2015) adopt a similar approach to deal with the uncertainties regarding renewables and variable loads in the operation of a MG. A Mixed-Integer Linear Programming (MILP) optimization model to design the energy infrastructure of a MG is presented in Bracco et al. (2018), where the objective function is defined to minimize the total costs related to RES power plants, ESSs and EV charging infrastructure and the costs related to the energy exchange with the public grid, in turn maximizing the net income. The model can be adopted to run the infrastructure as it suggests the operations of the BESS and EVs. Bartolucci et al. (2023) present a bi-level optimization approach where the upper optimization sizes the EV supply equipment, BESS capacity and Photovoltaic (PV) peak power of a charging station integrated with RESs and BESS using a Multi-Objective Genetic Algorithm, while a MILP algorithm is used in the lower optimization for the optimal scheduling of the charging process. A MILP-based optimization model is presented in Dukpa et al. (2022) where EV arrival and solar forecasts are modelled to maximize profitability of a RES integrated EV Charging Station (EVCS). A unitary cost is applied to limit the charge-discharge cycles of the BESS, in order to extend its operating life. Raghuveer et al. (2023) also adopt the method of adding a cost constraint to the BESS charge-discharge cycles in their MILP-based EMS, implemented under the rolling horizon approach for the management of a MG with

10.1016/j.ifacol.2024.07.109

EVCS integrated with RESs. Xiao et al. (2019) present a MILP-based EMS model for the optimization of a MG with shiftable and non-shiftable loads along with EVCSs fed by PV, Wind Turbines (WTs) and diesel generator. The objective of the EMS is to minimize costs of generation and penalties for load shifting; the Monte Carlo method is used to model the behaviour of EVs while Day-ahead scheduling of energy is done to minimize costs.

The present paper proposes a MILP-based EMS for the optimal day-ahead operation and scheduling of an EVCS facility currently connected to a wind farm. The site will soon include a commercial building, a rooftop PV system, and a BESS. The use of smart inverters for power plants permits to satisfy the reactive power demand of the charging hub, reducing the burden on the public network. The capability curves of the inverters of WTs, PV units, BESS and grid connection are modelled. The EMS is run over 24 hours, with a time resolution of one hour, with the objective of minimizing the operating costs. The novelty of this paper lies in the model application to a real facility and to the use of actual data from the wind farm and the EV chargers, besides the innovative approach for the linearization of WTs inverter's capability curves. The paper is organized as follows: Section 2 presents the mathematical model of the EMS; the case study and results are discussed in Section 3, while Section 4 draws the conclusions of the study.

2. MATHEMATICAL MODEL

The optimization horizon is subdivided into T time intervals of duration Δ. The objective of the EMS is to manage the RES plants to minimize the operating costs of the hub.

2.1 Rooftop PV Plant

The hub plans to increase the self-consumption of RES energy by installing a rooftop PV plant. To maximize the energy production from the PV plant, R sets of PV modules are installed according to each of the roof orientations of the commercial building present at the charging hub. The PV performance follows closely the relations presented by Evans et al. (1977) and Menicucci et al. (1989). These relations, along with the solar irradiance data from the Photovoltaic Geographical Information System (PVGIS) software, provide the available active power production from the PV plant, to be used as an input to the optimization problem. The PV inverter is sized at the rated capacity of the PV plant to avoid curtailment and to satisfy reactive power demand at hours when then the plant is not working at Maximum Power Point Tracking (MPPT). Given that the relation between the active power injected by the PV, P_t^{PV} and the inductive reactive power supplied by the PV inverter, $Q_t^{PV,out}$ would call for a capability curve with a semicircular operating range, that would introduce nonlinearity in the optimization problem, the capability curve of the PV inverter is linearized to have an hexagonal operating range with an approximation error of 7% as presented in Bracco et al. (2023). In formulas:

$$P_t^{PV} \leq A^{inv,PV} \tag{1}$$

$$0 \leq Q_t^{PV,out} \leq A^{inv,PV} \tag{2}$$

$$P_t^{PV} \leq -Q_t^{PV,out} + A^{inv,PV} * \sqrt{2} \tag{3}$$

where $A^{inv,PV}$ is the size of the PV inverter. The PV inverter operates in one quadrant as it is prevented from absorbing inductive reactive energy.

2.2 Wind Turbine Model

The active power production from the WTs follows their power curve and is used as an input of the EMS. Typically, wind farms adopt a u-shaped sigmoid capability curve as presented by Murphy et al. (2013), shown by the blue curve in Figure 1. The sigmoid introduces nonlinearity which can be resolved by linearizing the capability curve as shown by the area enclosed by the red curve in Figure 1.

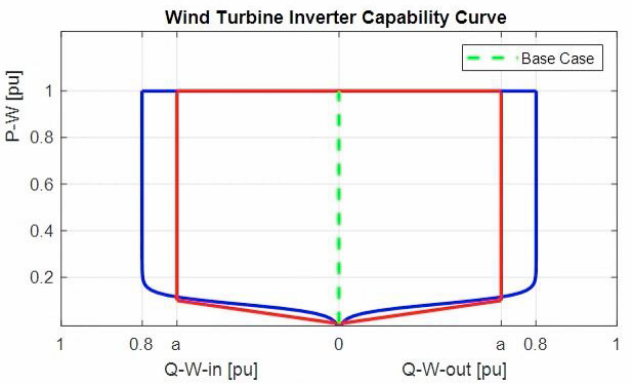

Figure 1. Typical Wind Farm Capability Curve (blue), Used Capability Curve of WT (red).

The WT inverter's capability curve is linearised as follows:

$$0 \leq P_t^W \leq P^{W,rated} \tag{4}$$

$$0 \leq Q_t^{W,out} \leq a * A^{inv,W} \tag{5}$$

$$0 \leq Q_t^{W,in} \leq a * A^{inv,W} \tag{6}$$

$$P_t^W \geq b * Q_t^{W,out} \tag{7}$$

where P_t^W is the active power production from the wind farm, $Q_t^{W,out}$ and $Q_t^{W,in}$ indicate the inductive reactive power supplied/absorbed by the WT inverter, $A^{inv,W}$ is the size of the WT inverter and a and b are two coefficients defined by the WT inverter manufacturer.

2.3 Grid Connection

The connection with the external public network serves multiple purposes: active and reactive power demand satisfaction in case of emergencies and revenue generation through sale of surplus production from RESs. The relations between the active power injected into the grid $P_t^{G,s}$, the active power absorbed from the grid $P_t^{G,b}$, the inductive reactive power absorbed from the grid $Q_t^{G,b}$ and the inductive reactive power injected to the grid $Q_t^{G,s}$ provide a circular capability curve of the main transformer that would again introduce nonlinearity in the optimization problem. Fresia et al. (2023) present the linearised constraints which have been adopted in this work. The EMS, with the help of binary variables $x_t^{G,s}$ and $x_t^{G,b}$, prevents the simultaneous sale and purchase of active energy from the public grid.

2.4 BESS

The energy content of the BESS E_t^B is governed by the energy balance that includes the charged and discharged active power, $P_t^{B,ch}$ and $P_t^{B,dch}$ respectively, and takes also into account the self-discharge coefficient λ, and the charging and discharging efficiencies, η_{ch}^B and η_{dch}^B respectively. Both $P_t^{B,ch}$ and $P_t^{B,dch}$ are limited by the size of the BESS inverter $A^{inv,B}$. The related constraints are reported below.

$$E_{t+1}^B = (1-\lambda) * E_t^B + \Delta * \left(\eta_{ch}^B * P_t^{B,ch} - \frac{P_t^{B,dch}}{\eta_{dch}^B}\right) \quad (8)$$

$$0 \leq P_t^{B,ch} \leq A^{inv,B} * x_t^{B,ch} \quad (9)$$

$$0 \leq P_t^{B,dch} \leq A^{inv,B} * x_t^{B,dch} \quad (10)$$

$$x_t^{B,ch} + x_t^{B,dch} \leq 1 \quad (11)$$

$$SOC^{min} * C^B \leq E_t^B \leq SOC^{max} * C^B \quad (12)$$

$$x_t^{B,ch} + x_t^{G,b} \leq 1 \quad (13)$$

$$x_t^{B,dch} + x_t^{G,s} \leq 1 \quad (14)$$

In (9) and (10), binary variables $x_t^{B,ch}$ and $x_t^{B,dch}$ denote the status of operation of the BESS and (11) prevents the simultaneous charging/discharging of the BESS. The BESS is always maintained between a minimum and maximum state of charge to extend life of operation. In (12), SOC^{min} and SOC^{max} are the minimum and maximum state of charge of the BESS respectively, while C^B is the rated capacity of the BESS. Equations (13) and (14) are additional constraints that can be used to prevent the EMS from charging the BESS with active energy purchased from the network and discharging the BESS only to increase the sale of active energy to the network. This can be viewed as a method to avoid unnecessary charge/discharge cycles to increase the operating life of the BESS.

The BESS inverter and the grid connected transformer share a similar circular capability curve which allows to adopt similar constraints to simplify the model. While Lazzeroni et al. (2019) only use a portion of the operating range of the circular capability curve of the BESS, Fresia et al. (2023) provide an octagonal capability curve with linearised constraints to avoid nonlinearity in the optimization problem. Assuming that the BESS inverter does not absorb any inductive reactive power, its capability curve is described by:

$$0 \leq Q_t^{B,out} \leq A^{inv,B} \quad (15)$$

$$P_t^{B,ch} \leq -Q_t^{B,out} + A^{inv,B} * \sqrt{2} \quad (16)$$

$$P_t^{B,dch} \leq -Q_t^{B,out} + A^{inv,B} * \sqrt{2} \quad (17)$$

where $A^{inv,B}$ is the size of the BESS inverter and $Q_t^{B,out}$ is the inductive reactive power injection by the BESS inverter.

2.5 Electric Power Balances

Both the active and reactive power demand of all the electric loads of the hub needs to be satisfied at all time intervals by the available technologies or by the external grid. In formulas:

$$P_t^{El} + P_t^{EV} + P_t^{B,ch} + P_t^{G,s} = P_t^{G,b} + P_t^{B,dch} + P_t^{W} + P_t^{PV} \quad (18)$$

$$Q_t^{El} + Q_t^{G,s} = Q_t^{G,b} + Q_t^{B,out} + Q_t^{W,out} + Q_t^{PV,out} \quad (19)$$

where P_t^{El} and P_t^{EV} respectively are the active power demand of the commercial building and of the EVs present at the hub, while Q_t^{El} is the reactive power demand of the building.

2.5 Objective Function

The objective function of the EMS is defined to minimize the operating costs of the charging hub related to the exchange of active power with the public network. In formulas:

$$Obj = \Delta * \sum_{t=1}^{T} (OC_t - R_t) \quad (20)$$

$$OC_t = P_t^{G,b} * p_t^{G,bP} + Q_t^{G,b} * p_t^{G,bQ} + Q_t^{G,s} * r_t^{G,sQ} \quad (21)$$

$$R_t = P_t^{G,s} * r_t^{G,s\_P} \quad (22)$$

where OC_t refers to the operating costs of the hub related to the absorption of active and reactive power from the public network, while R_t represents the revenues generated from the sale of active power to the public network. $p_t^{G,bP}$ and $p_t^{G,bQ}$ are the unit costs of active and reactive power absorption from the network in €/kWh and €/kVARh respectively and $r_t^{G,sP}$ is the unit revenue generated from the active power injection into the network in €/kWh. The injection of reactive power to the public network is penalized using $r_t^{G,sQ}$ in €/kVARh.

3. RESULTS

This section provides a description of the facility and of the input data, before discussing the optimization results.

3.1 Site Description

The EVCS under study was launched by RICARICA s.r.l. (from now on, "RICARICA"), a division of FERA s.r.l. (from now on, "FERA"), in June 2023 in Vado Ligure, a small town in the Ligurian region of Italy. The EVCS is directly connected to a wind farm, owned by FERA, installed some kilometres away. The facility supports EV chargers owned by both RICARICA and a second operator, that for confidentiality reasons, from now on, will be called "Operator 2". Plans to build an energy-efficient building at the site are already in motion. The building is expected to host FERA's offices along with commercial retail outlets. A PV plant of 400 kWp is to be installed on the rooftop of the new building, along with a 1.1 MWh BESS system to provide flexibility. $A^{inv,PV}$ is equal to 400 kVA and $A^{inv,B}$ is equal to 1.1 MVA. The wind farm connected to the hub consists of 4 Enercon E-92 WTs, each with a rated power of 2.35 MW, bringing the total capacity to 9.4 MW. $A^{inv,W}$ is equal to 9.4 MVA; a and b coefficients describing the inverter's capability curve in (5)-(7) are respectively equal to 0.77 (p.u. on local base) and 0.13. At present, a total of three EV chargers owned by RICARICA are present at site, two of which have an output power of 350 kW; the third has a rated output of 75 kW. The 350 kW ultra-fast chargers can charge electric trucks, light duty vehicles and cars. The twelve EV chargers owned by Operator 2 have a

rated output of 250 kW each. The new building is modelled to have inductive loads while the EVs using the facility are modelled as purely resistive loads. The hub is connected to the external network through a Medium Voltage (MV) connection with a 12 MVA transformer. Active energy taken from the grid is charged at the hourly tariffs according to the time bands, while active energy fed into the grid is charged at Prezzo Unico Nazionale (PUN – *the Italian Day-Ahead Electricity Market Clearing Price*). The reactive power absorption/injection from/to the network is penalized, if applicable, according to the tariffs established by the Italian Regulatory Authority for Energy, Networks and Environment (ARERA). A simplified layout of the charging hub is shown in Figure 2.

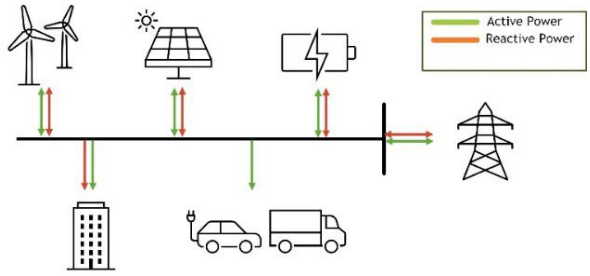

Figure 2. Simplified layout of the charging hub.

3.2 EV and Building Demand Estimation

The EV demand is used as an input to the EMS and is predicted on the basis of current and forecasted EV sales, using the annual active energy absorbed by EVs at the hub for the previous operating year and the hourly, daily and monthly EV arrival factors: these factors, provided by RICARICA, describe for each hour the percentage of EVs charging at the EVCS out of the total number of users in the previous operating year. In this way, the EV demand can be forecasted for all the upcoming years, considering the forecasted increase in EV sales. The load profile of the building has been estimated from the available ones of the latest Typical Meteorological Year (TMY3) locations in the United States, considering a similar building, using the total floor area and the "Koppen-Gieger" classification system.

3.3 Optimal Results

The referenced relations along with the equations (1) - (22) translate the optimization problem into a MILP problem. Gurobi solver along with Yalmip toolbox has been used to solve the MILP problem, implemented in Matlab R2020b. Given the irregularity on the availability of RESs and the rising trends in the sale of EVs, four scenarios regarding the availability of RESs and current and forecasted load demands of the hub are defined. Two typical days are selected corresponding to high and low active power production from the RESs. The EMS optimizes the operation of the hub either considering the present (year 2023) and the future forecasted (year 2031) EV and load scenarios, for both typical days. The scenarios are reported in Table 1.

Scenario I deals with the operation of the hub when the active power production from RESs is almost at full capacity, while the hub satisfies the present EV and building demand. The combined active power production from RES power plants is, at MPPT, about 125 times the combined load demand and therefore, for the whole day, excess active energy is sold, as shown in Figure 3a. Scenario II describes the operation of the hub under increased EVs and building demands. The active power output from RES plants is in excess in this scenario as well, as shown in Figure 3b: there is no need for absorption of active energy from the external network. It can be noted that in both Scenario I and Scenario II, the BESS is rarely used, given the surplus production from RES plants.

Table 1. Characterization of the scenarios

Scenario	RES Production	Total Demand
I	High	Present
II	High	Future
III	Low	Present
IV	Low	Future

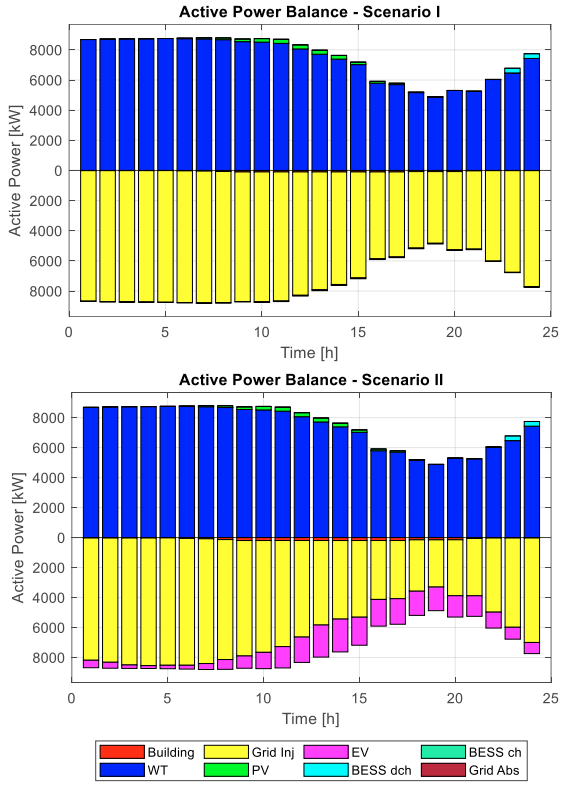

Figure 3. (a) Active power balance in Scenario I (top). (b) Active power balance in Scenario II (bottom)

Scenario III considers the operation of the hub under the present-day load demand on a typical day when the active power output from the RES plants is lower than the total load demand. It can be noted from Figure 4a that, at times when the technologies at the site cannot satisfy the local active power demand, active energy is bought from the public grid. From Figure 4a, it is interesting to note that to reduce the operating costs the EMS charges the BESS with active energy bought from the external grid and discharges the BESS at a later instant to increase the sale of active energy to the grid, thereby increasing the revenues. Figure 4a points out a glaring issue of the model for the operation of the BESS. Given that in Scenario III the RES production is insufficient to satisfy the active energy demand, active energy is absorbed from the grid for demand satisfaction. The BESS charges from the active energy absorbed from the network and later discharges the energy to be injected to the grid to increase the revenues. If not

constrained, there will be a larger number of charge/discharge cycles which leads to cycle aging and capacity deterioration of BESS. When the BESS is prohibited from charging using active energy absorbed from the grid and is prohibited from discharging to increase the sale of active energy to generate revenue, the number of charge/discharge cycles is significantly reduced as shown in Figure 4b and there is a significant difference in the amount of active energy exchanged between the hub and the public grid. Even in this constrained condition, at some time intervals the hub can sell excess active energy from RESs: in these intervals, the local load demand is lower than the combined active RES power output. The BESS is not charged to reduce the hub operational costs, as shown in Figure 4b. Figure 4c shows the active power balance of the hub in Scenario IV with increased load demand and low RES production. It can be noticed that, barring a few time intervals, the active power demand is satisfied by energy bought from the grid since, on the selected day, the active power production from RES power plants cannot fully satisfy the active power demand of the hub.

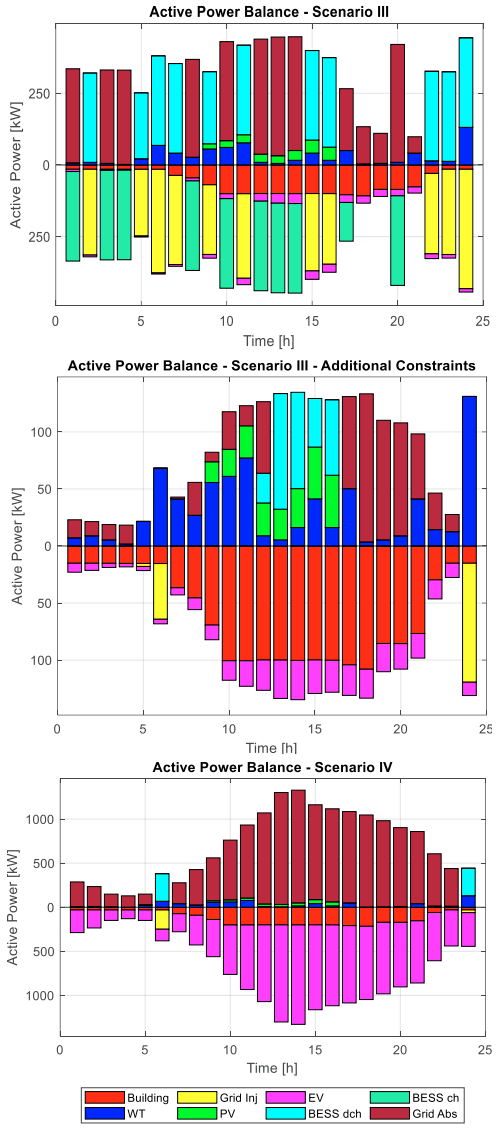

Figure 4. (a) Active power balance in Scenario III (top). (b) Active power balance in Scenario III with additional constraints (centre). (c) Active power balance in Scenario IV (bottom).

The external grid compensates for the unsatisfied demand, increasing the operational costs. In this scenario, the additional constraints (13) and (14) have minimal effect on the operation of the BESS, due to the presence of a higher unsatisfied demand: therefore, relevant results are not reported. Regarding the reactive power balance, in all the four scenarios, to avoid penalties, the EMS allocates the RES inverters to satisfy the demand. Figure 5 depicts the reactive power balance in Scenario II where the RES inverters are deployed for reactive power satisfaction.

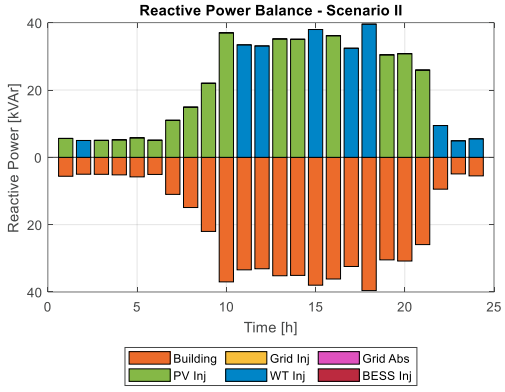

Figure 5. Reactive power balance of the hub in Scenario II

3.4 Discussion

The energy results of the optimization for each scenario are summarized in Table 2. For confidentiality, they are expressed in per unit on the base of the total energy demand of the facility, given by the sum of $E^{El,a}$ and E^{EV}, that respectively represent the active energy demand of the building and of the EVs. $E^{El,r}$ represents the reactive energy requested by the building. In Scenarios I and II, where the combined share of active energy output from the PV plant and the wind farm ($E^{PV,a}$ and $E^{W,a}$ respectively) exceeds the total active energy requested, there is no purchase of active energy from the public grid ($E^{G,b,a}$), while the excess active energy is sold to the public grid ($E^{G,s,a}$) to increase the revenues, thereby reducing the net costs of the hub. In Scenarios III and IV, active energy is bought from the grid only to compensate the combined deficit in energy output from the RES plants and the BESS. It is interesting to note that in Scenario III, the net costs are lower when the additional constraints on the operation of the BESS are not applied: it is therefore up to the system operator to decide whether to implement these restrictions or not. Another important observation is that, to avoid additional costs, the reactive energy requested by the building is always satisfied by the WT and the PV inverters ($E^{W,r}$ and $E^{PV,r}$). The absorption of reactive energy from the external network $E^{G,b,r}$ is notably at small values, as it is only at time intervals when there are no penalties in place for reactive energy absorption from the grid. To prevent the hub from incurring any penalties, reactive energy injection into the grid is avoided ($E^{G,s,r}$). Using the CO_2 emission factor for the national grid as reported by Italian Institute for Environmental Protection and Research (2023) and knowing the active energy absorbed from the network in each scenario, it is possible to calculate the CO_2 emissions related to the energy absorbed from the grid. Table 3 presents a comparison between the amount of CO_2 emissions for each scenario in relation to the active energy absorption

from the public network before and after the integration of RESs in the charging hub. In Table 3, Em^{bf} represents the CO_2 emissions from the grid related to the absorption of active energy by the hub for the demand satisfaction without any contribution from RESs/BESS while Em^{af} represents the CO_2 emissions from the grid related to the absorption of active energy by the hub to compensate for the deficit in active energy output from RESs/BESS for the load demand request. Even with an increased load demand, the presence of RESs in the hub has been effective in reducing CO_2 emissions.

Table 2. Energy quantities related to the hub.

Scenario	I	II	III	IV
$E^{El,a}$	0.64	0.10	0.78	0.18
E^{EV}	0.36	0.90	0.22	0.82
$E^{W,a}$	80.32	6.12	0.40	0.04
$E^{PV,a}$	0.95	0.07	0.13	0.02
$E^{B,ch}$	0	0	1.57	0
$E^{B,dch}$	0.27	0.02	1.77	0.04
$E^{G,b,a}$	0	0	2.03	0.92
$E^{G,s,a}$	80.56	5.22	1.73	0.02
$E^{El,r}$	1	1	1	1
$E^{W,r}$	0.69	0.51	0.50	0.21
$E^{PV,r}$	0.30	0.458	0.50	0.79
$E^{B,r}$	0	0	0	0
$E^{G,b,r}$	0.01	0.01	0	0
$E^{G,s,r}$	0	0	0	0

Table 3. Grid CO2 emissions with and without RES utilization.

Scenario	I	II	III	IV
Em^{bf} [kg]	574.49	7,537.32	487.54	4,260.92
Em^{af} [kg]	0	0	189.39	3,849.07
Change [%]	100	100	61.15	9.67

4. CONCLUSIONS

The present paper aimed to develop an EMS model based on MILP for the day ahead scheduling of the optimal operation of an EV charging hub directly fed by a wind farm. The developed model was able to optimize the operations of the hub considering different scenarios of the available local active power production. The CO_2 emissions related to the absorption of active energy by the hub from the grid can be considerably reduced by including RES plants at site. While the inclusion of RESs serves two additional purposes, generating revenues through the sale of excess active energy to the public grid as well as reactive power demand satisfaction by the RES inverters to avoid incurring any penalties, the inclusion of BESS helps to bypass the irregularity in RES availability thereby reducing the operating costs. The model can be worked upon to include several other aspects such as the effects of battery degradation in the BESS model, investigate the possibility of smart charging of light and heavy vehicles present at the facility for overnight charging also exploiting the Vehicle-to-Grid functionality. Further studies can also include the real-time optimization of the hub when the EV demand deviates from the forecasted values.

REFERENCES

Bartolucci, L. et al. 2023. PV assisted electric vehicle charging station considering the integration of stationary first- or second-life battery storage. *Journal of Cleaner Production* 383.

Bracco, S., Cancemi, C., Causa, F., Longo, M., & Siri, S. 2018. Optimization model for the design of a smart energy infrastructure with electric mobility. *IFAC-PapersOnLine* 51(9): p.200–205.

Bracco, S., Delfino, F., Pampararo, F., Robba, M., & Rossi, M. 2015. A dynamic optimization-based architecture for polygeneration microgrids with tri-generation, renewables, storage systems and electrical vehicles. *Energy Conversion and Management* 96: p.511–520.

Bracco, S., & Fresia, M. 2023. Energy Management System for the Optimal Operation of a Grid-Connected Building with Renewables and an Electric Delivery Vehicle. *EUROCON 2023 - 20th International Conference on Smart Technologies, Proceedings*: p.472–477.

Dukpa, A., & Butrylo, B. 2022. MILP-Based Profit Maximization of Electric Vehicle Charging Station Based on Solar and EV Arrival Forecasts. *Energies* 15(15).

European Environment Agency. 2022. Digitalisation in the mobility system: challenges and opportunities.

Evans, D.L., & Florschuetz, L.W. 1977. Cost studies on terrestrial photovoltaic power systems with sunlight concentration. *Solar Energy* 19(3): p.255–262.

Fresia, M., & Bracco, S. 2023. Electric Vehicle Fleet Management for a Prosumer Building with Renewable Generation. *Energies* 16(20): p.7213.

Italian Institute for Environmental Protection and Research. 2023. Efficiency and decarbonization indicators in Italy and in the biggest European Countries.

Lazzeroni, P., & Repetto, M. 2019. Optimal planning of battery systems for power losses reduction in distribution grids. *Electric Power Systems Research* 167: p.94–112.

Menicucci, D.F., & Fernandez, J.P. 1989. User`s manual for PVFORM: A photovoltaic system simulation program for stand-alone and grid-interactive applications.

Murphy, C., & Keane, A. 2013. Optimisation of wind farm reactive power for congestion management. *2013 IEEE Grenoble Conference PowerTech, POWERTECH 2013*.

Pan, X., Niu, X., Yang, X., Jacquet, B., & Zheng, D. 2015. Microgrid energy management optimization using model predictive control: a case study in China. *IFAC-PapersOnLine* 48(30): p.306–311.

Raghuveer, R.M., Bhalja, B.R., & Agarwal, P. 2023. Real-Time Energy Management of EVs in a Microgrid Integrated with Distributed Energy Resources Considering Uncertainties. *2023 IEEE 3rd International Conference on Sustainable Energy and Future Electric Transportation, SeFet 2023*.

Tant, J., Geth, F., Six, D., Tant, P., & Driesen, J. 2013. Multiobjective battery storage to improve PV integration in residential distribution grids. *IEEE Transactions on Sustainable Energy* 4(1): p.182–191.

Xiao, Z., Li, Hui, Zhu, T., & Li, Huaimin. 2019. Day-ahead optimal scheduling strategy of microgrid with EVs charging station. *PEDG 2019 - 2019 IEEE 10th International Symposium on Power Electronics for Distributed Generation Systems*: p.774–780.